Available online at www.sciencedirect.com
ScienceDirect
Journal of Molecular Structure 889 (2008) 28–34
Journal of MOLECULAR STRUCTURE
www.elsevier.com/locate/molstruc

Spectroscopic properties and cyclic voltammetry on a series of meso-tetra(*p*-alkylamidophenyl)porphyrin liquid crystals and their Mn complexes

Erjun Sun [a], Yuhua Shi [a], Ping Zhang [a], Mi Zhou [b], Yihua Zhang [a], Xuexin Tang [a], Tongshun Shi [a,*]

[a] *College of Chemistry, Jilin University, Jiefang Road 2519, Changchun 130023, PR China*
[b] *College of Physics, Jilin University, Jiefang Road 2519, Changchun 130023, PR China*

Received 12 September 2007; received in revised form 2 January 2008; accepted 9 January 2008
Available online 17 January 2008

Abstract

A series of meso-tetra(*p*-alkylamidophenyl)porphyrin ligands and their manganese(III) complexes are reported in this paper. The mesomorphism was investigated by differential scanning calorimetry (DSC) and polarized optical microscopy (POM) and the results show that only the porphyrin ligands with long side chains show liquid crystalline behavior, and they exhibit a high phase transition temperature and a broad mesophase temperature span. Furthermore, we investigated the properties of the compounds by means of UV−vis spectra, infrared spectra, Resonance Raman spectra, fluorescence spectra, thermal analysis and cyclic voltammetry. These studies indicate that the length of side chains has little effect on the properties of porphyrin compounds. According to thermal studies, the decomposition of porphyrin ligand and Mn complex is a continuous process.

Keywords: Porphyrins; Mn complexes; Liquid crystal; Cyclic voltammetry; Thermal analysis

1. Introduction

Porphyrins and metalloporphyrins have received extraordinary attention in recent years for using these compounds in photodynamic therapy [1], optoelectronic devices [2], sensors [3], molecular logic devices [4], and artificial solar energy harvesting and storage schemes [5]. The porphyrin skeleton has an extended π-conjugation system [6], leading to a wide range visible light absorptions and p-type properties as an electronic system. Thus, the control of orientation of porphyrin chromophores can play a very important role.

Porphyrin liquid crystal is an important member of the liquid crystals family. The first liquid crystalline porphyrin derivative was reported by Goodby et al. in 1980 [7]. Since then, many mesogenic porphyrins have been synthesized and their mesomorphic properties were investigated [8–12]. But up to now, most of the side chains of TPP derivative liquid crystals are alkyl, alkoxy, or acyloxy group, those bearing the alkylamido group as side chains porphyrin liquid crystals have been reported little [13]. In this paper, a series of 5,10,15,20-tetra(*p*-alkylamidophenyl)porphyrin ligands and their Mn complexes were synthesized and their liquid crystal properties were studied firstly (the structures are shown in Fig. 1). The mesomorphism studies show that only the ligands with long chains of more than 12 carbon atoms have liquid crystalline behavior, while the Mn complexes are not liquid crystals. Furthermore, we have investigated these compounds by Resonance Raman spectra, cyclic voltammetry, thermal studies and fluorescence spectroscopy. These studies will provide wider ground for choice and application of the materials.

* Corresponding author. Tel./fax: +86 431 85168898.
E-mail address: sunerjun1974@hotmail.com (T. Shi).

0022-2860/$ - see front matter © 2008 Elsevier B.V. All rights reserved.
doi:10.1016/j.molstruc.2008.01.014

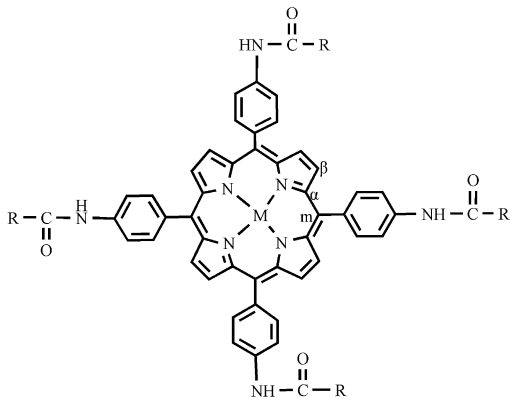

M=2H, Mn(Cl)
R=C_nH_{2n+1},
Ligands, n = 7, 9, 11, 13, 15, 17 correspond to 8L, 10L, 12L, 14L, 16L and 18L, respectively; Mn complexes, n =7, 9, 11, 13, 15, 17 correspond to 8Mn, 10Mn, 12Mn, 14Mn, 16Mn and 18Mn, respectively.

Fig. 1. The structures of porphyrin ligands and their Mn complexes.

2. Experimental

2.1. Materials and methods

UV−vis spectra were collected on a Shimadzu UV-240 spectrometer in the region of 350−700 nm using DMF as solvent. Infrared spectra were recorded on a Nicolet 5PC-FT-IR spectrometer using KBr pellets in the region of 4000−400 cm^{-1}. Raman spectra were recorded with a Renishawinvia Raman spectrophotometer equipped with an integral microscopy. Radiation of 514.5 nm was obtained from an Ar^+ laser. Redox potentials of the compounds (10^{-3} mol/L) in dried DMF containing 0.1 mol/L TBAP as supporting electrolyte were determined at room temperature by cyclic voltammetry with a CHI 660A electrochemical analyzer using a three-electrode system under deaerated conditions. Platinum button and platinum wire were served as working and counter electrodes, respectively. The reversibility of the electrochemical processes was evaluated by standard procedures, and all potentials were recorded against an Ag/Ag^+ reference electrode (0.01 mol/L $AgNO_3$ in acetonitrile (CH_3CN) solution). Thermal analysis were recorded on TGA and DTA apparatus (sample: 3−4 mg, heating rate: 10 °C/min, and atmosphere: static air). The differential scanning calorimetry (DSC) was performed with a Perkin-Elmer 7 series thermal analysis system at a scan rate of 10 °C/min under nitrogen flow. Optical microscopical properties were observed by a XinTian XP1 (CCD: TOTA-500 II) polarized light microscope, equipped with a variable temperature stage (Linkam TMS 94). The fluorescence spectra were recorded with a SPEX Fluorolog-2T2 spectrofluorometer (450-W xenon lamp as the excitation source) and obtained from 10^{-5} mol/L DMF solution in 1 × 1 × 5 cm fluorescence cells at room temperature. The quantum yields of porphyrins were estimated from the emission and absorption spectra by a comparative method using the following equation [14]:

$$\Phi_{\text{sample}} = \Phi_{\text{TPPZn}}(F_{\text{sample}}/F_{\text{TPPZn}})(A_{\text{TPPZn}}/A_{\text{sample}})$$

Where F_{sample} and F_{TPPZn} are measured fluorescence integral areas (under the fluorescence spectra) of the sample and the reference TPPZn, respectively. A_{sample} and A_{TPPZn} are the absorbance of the sample and the reference. Φ_{sample} and Φ_{TPPZn} ($\Phi_{\text{TPPZn}} = 0.033$ [15]) are the quantum yields of the sample and the reference TPPZn at same excitation wavelength. The effect of solvent is neglect.

All reagents and solvents were of the commercial reagent grade and were used without further purification except DMF was predried over activated 4 Å molecular sieve and vacuum distilled from calcium hydride (CaH_2) prior to use. The dry CH_3CN was obtained by redistillation from CaH_2.

2.2. Preparation of porphyrin ligands and Mn complexes

2.2.1. Synthesis of 14L

14L was prepared by the reaction of the 5,10,15,20-tetra (4-aminophenyl)porphyrin ($TAPPH_2$) which was synthesized in our laboratory according to the method of Kruper [16] with myristyl chloride. $TAPPH_2$ (1.00 g) was dissolved in freshly distilled $CHCl_3$ (150 ml), and triethylamine (2 ml) was added. A solution of myristyl chloride (2.8 ml) in $CHCl_3$ (10 ml) was added drop wise to the above solution within 2 h with stirring at 70 °C. The reaction solution then was refluxed for 8 h and cooled to room temperature. Then 200 ml distilled water was added to the reaction mixture and extracted three times by equal volumes of freshly distilled chloroform. The chloroform solution was concentrated and applied to a silica gel column, and the column was eluted with $CHCl_3$—C_2H_5OH (9:1, V/V). The first band was collected and condensed. The precipitated product was crystallized from chloroform and ethanol and was obtained as purple solid. Yield: 38.0%. ^1H NMR (DMSO-d_6, 500 Hz): δ 8.863 (s, 8H, pyrrole ring), 10.308 (s, 4H, —NH—CO—), 8.050–8.137 (m, 16H, benzene ring), 1.713–1.742 (t, 8H, —CO—CH_2—), 1.271–1.419 (m, 88H, alkyl CH_2), 0.829–0.856 (t, 12H, alkyl CH_3), −2.898 (s, 2H, pyrrole N–H). Elemental analysis: calc. for $C_{100}H_{138}N_8O_4$: C 79.21, H 9.17, N 7.39; Found: C 79.29, H 9.11, N 7.34.

2.2.2. Synthesis of 14Mn

The complex 14Mn was prepared by the reaction of 14L (0.20 g) with $MnCl_2\cdots 4H_2O$ (2.00 g) in $CHCl_3$ (20 ml) and DMF (20 ml) mixture at 70 °C under the protection of nitrogen stream for about 3 h. The extent of the reaction was monitored by measuring the UV–vis spectrum of the reaction solution. The reaction mixture then was chromatographed on silica gel column (eluent: $CHCl_3$—C_2H_5OH 9:1) and crystallized from chloroform and ethanol. Yield: 80.3%. Elemental analysis: calc. for $C_{100}H_{136}N_8O_4MnCl$: C 74.85, H 8.54, N 6.98; Found: C 74.77, H 8.61, N 6.95.

The preparation methods and results of other ligands and Mn complexes are similar to those mentioned above.

3. Results and discussion

3.1. Liquid crystals

The crystalline phase is characterized by DSC and the results show that only the ligands of 12L, 14L, 16L and 18L are liquid crystals while the 8L, 10L and all the Mn complexes are not. The calorimetric data of porphyrin liquid crystals are shown in Fig. 2 and the transition temperatures and enthalpies of the porphyrin ligands are given in Table 1. From Fig. 2 and Table 1, we can see that each of the ligands shows one or two mesophases. The porphyrin ligands show a high transition temperature and a broad mesophase temperature span. The lowest temperature for the transition from crystal to liquid–crystal phase is 115 °C (18L) and the highest is 182 °C (12L). The broadest mesophase temperature span is 160 °C (16L and 18L) and the narrowest is 78 °C (12L). With increasing the side chain length, the mesophase temperature span increased and the transition temperature decreased. The optical texture was observed by viewing the birefringence of the samples between crossed polarizers in a polarizing microscope. Fig. 3 shows the birefringence texture micrograph of 16L.

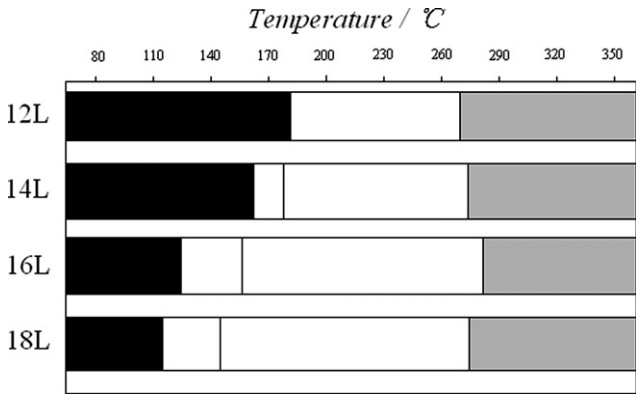

Fig. 2. Differential scanning calorimetry of 12L, 14L, 16L and 18L. Black, solid phase; white, mesophase; gray, isotropic.

Table 1
Calorimetric data for compounds 12L, 14L, 16L and 18L

Compound	T/ °C (ΔH/(KJ mol^{-1}))[a]	ΔT/ °C[b]
12L		
Heating	C[c] 182 (10.52) D[d] 270 (41.96) I[e]	88
Cooling	I 252 (−50.52) D 174 (−13.53) C	78
14L		
Heating	C 163 (25.36) D_1 177 (10.80) D_2 274 (57.31) I	111
Cooling	I 246 (−54.47) D_2 173 (−23.72) D_1 155 (−15.64) C	91
16L		
Heating	C 121 (3.66) D_1 156 (77.59) D_2 281 (77.36) I	160
Cooling	I 265 (−46.14) D_2 148 (−43.71) D_1 112 (−3.64) C	153
18L		
Heating	C 115 (4.20) D_1 143 (67.91) D_2 275 (57.09) I	160
Cooling	I 251 (−53.99) D_2 131 (−57.94) D_1 106 (−4.44) C	145

[a] Heating rate 10 °C min^{-1}, cooling rate 10 °C min^{-1}.
[b] Temperature range of liquid crystal.
[c] Crystal.
[d] Discotic mesophase.
[e] Isotropic liquid.

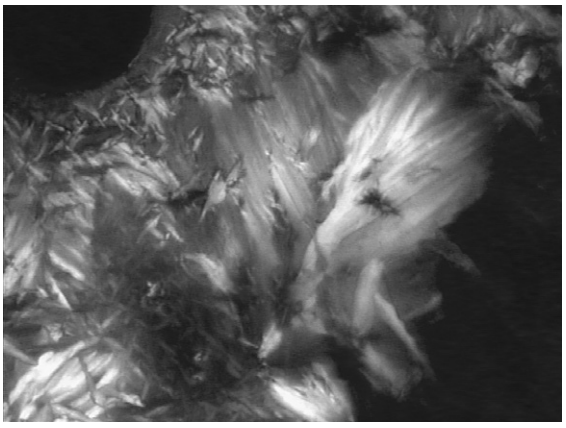

Fig. 3. Optical texture of 16L, cooling from the isotropic state.

Unlike porphyrin ligands, the Mn complexes show none of the liquid crystal behaviour. As we know, most discotic liquid crystals have a molecular structure that consists of a flat central core with several flexible chains placed around the outside edge of the core. But there is non-coplanarity of Mn complexes because of the axis coordination. This structure is unfavorable for the whole macromolecule to pack closely to form liquid crystal. On the other hand, the self-assemble of the metal porphyrins may be another reason. The amide N of the side chains may coordinate to the metal ion of the metal porphyrin which forms complicated multi-porphyrin aggregation.

3.2. UV–vis spectra

Fig. 4 shows the absorption spectra of 8L and 8Mn. As we know, the UV–vis absorption bands of the porphyrins are due to the electronic transitions from the ground state (S_0) to the two lowest singlet excited states S_1 and S_2 [17]. The $S_0 \rightarrow S_1$ transition gives rise to the weak Q bands in visible region while $S_0 \rightarrow S_2$ transition produces the strong Soret band in near UV region. In this work, the absorption bands of the 8L appear at 425, 520, 555, 595 and 650 nm. Compared with the ultraviolet characteristic absorption peak of TPP [18], the ultraviolet absorption peaks of porphyrin ligands show red shift. It is possibly because the *para*-alkylamidoyl group on the phenyl group of the meso-position of porphyrin ring is a donating electronic group, it enables the electronic density on the phenyl ring to strengthen, thus the phenyl ring conjugates with porphyrin macrocycle to a certain degree, this kind of conjugation action causes electron transition energy of the porphyrin

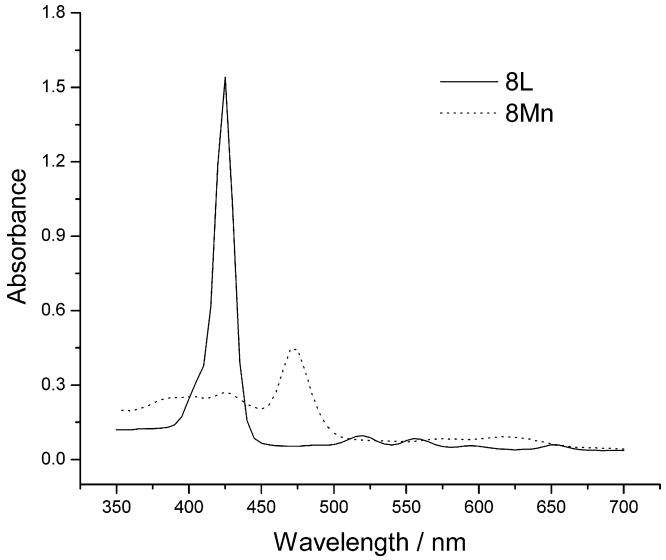

Fig. 4. The UV–vis spectra of 8L and 8Mn.

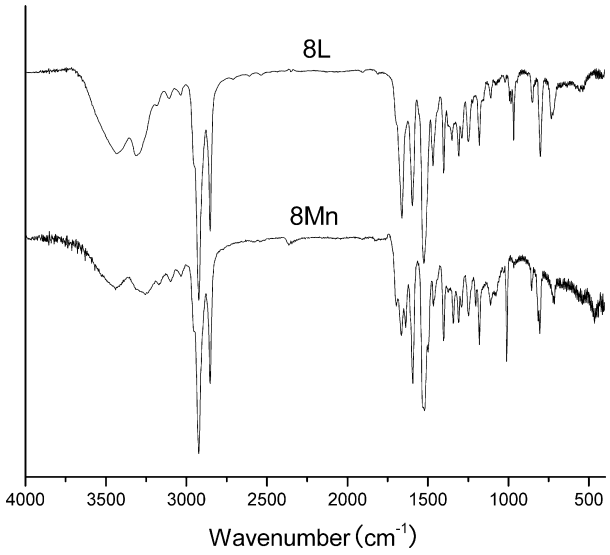

Fig. 5. The IR spectra of 8L and 8Mn.

macrocycle to reduce, making its ultraviolet absorption peak red shift. The 8Mn complex has an intense Soret band at 470 nm, with additional bands at 400, 425, 520, 570, 615 nm and the spectra patterns are similar to those of the five-coordinated Mn porphyrin complexes [19]. After the metal ion coordinated to porphyrin, the number of Q band decreases and the absorption frequencies shift because of the increasing of molecular symmetry. The spectra shapes and peak positions of other porphyrin ligands and Mn complexes are similar to those we mentioned above which shows that the length of side chains has little effect on the absorption spectra.

3.3. Infrared spectra

The IR bands at 3313–3318 cm^{-1}, 966–968 cm^{-1} of porphyrin ligands are due to the N—H stretching and bending vibration of the porphyrin core, but they disappear in the Mn complexes because the hydrogen atom in the N—H bonding is replaced by metal ion [20]. In addition, a new band appears at about 1011 cm^{-1} in the IR spectrum of Mn complexes, which is the characteristic of porphyrin metallation. The bands at about 3300 cm^{-1} of Mn complexes are assigned to N–H stretching vibration of amide group on the side chains, but in porphyrin ligands, they are combined with the N—H stretching of the porphyrin core and cannot been distinguished. The bands of the compounds at about 2850 and 2920 cm^{-1} are assigned to C—H stretching vibration. The bands in the range of 1658–1666 cm^{-1} are assigned to C=O stretching vibration (amide I) and the bands in the range of 1519–1535 cm^{-1} are assigned to N—H in-plane bending (amide II). The bands at 717–721 cm^{-1} are assigned to the methylene in-plane rocking vibration of straight alkyl chain including over four carbons. The IR spectra of 8L and 8Mn are shown in Fig. 5.

3.4. Resonance Raman spectra

The resonance Raman spectra of porphyrin ligands and Mn complexes using 514.5 nm excitation are shown in Figs. 6 and 7. The Resonance Raman spectra of tetraphenylporphyrin derivatives have been studied extensively [21–23]. Thus, the assignments of Raman bands of porphyrin ligands and Mn complexes are discussed briefly here. The wavenumber positions of vibration bands in the high-frequency region (900–1600 cm^{-1}) are sensitive to the core size, axial ligation and electron density of the central metal ion. In this region, the 1552 cm^{-1} band of porphyrin ligands is assigned to C_β–C_β stretch ν_2, which is up-shifted to 1570 cm^{-1} in Mn complexes. The band at about 1493 cm^{-1} of porphyrin ligands is assigned to the vibration

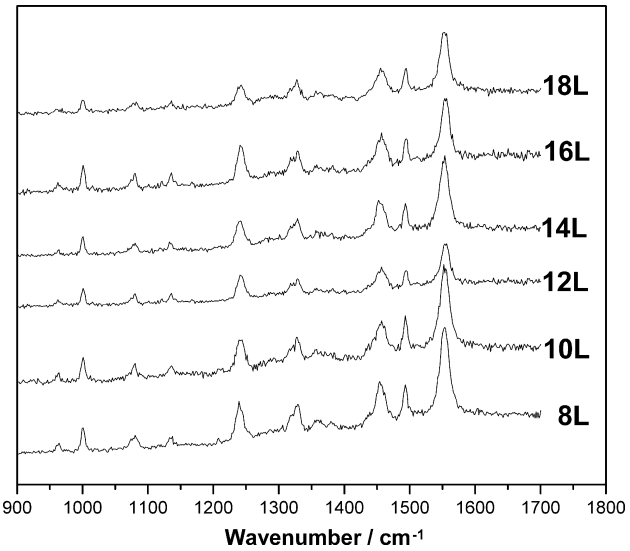

Fig. 6. Raman spectra of porphyrin ligands in 900–1700 cm^{-1} region with excitation wavelength at 514.5 nm.

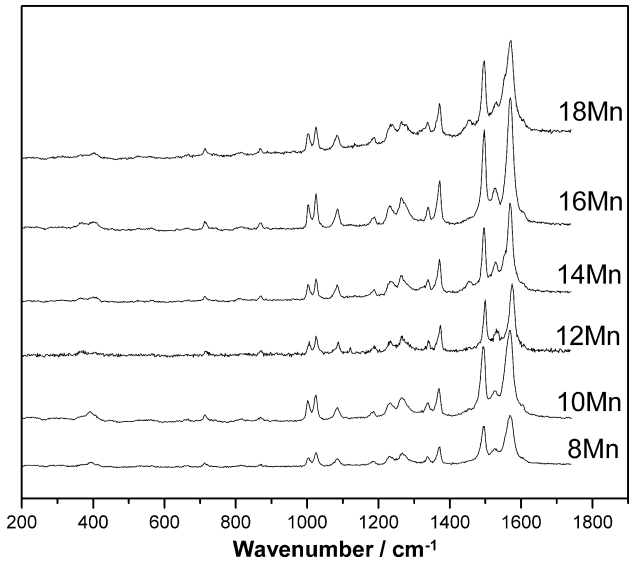

Fig. 7. Raman spectra of Mn complexes in 200–1700 cm^{-1} region with excitation wavelength at 514.5 nm.

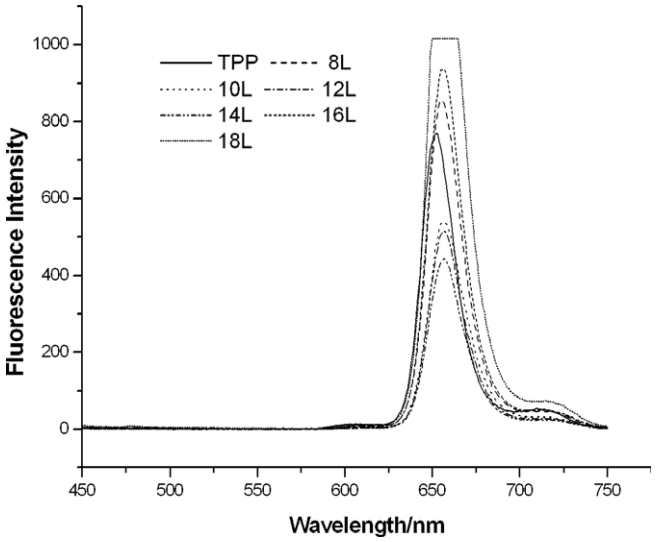

Fig. 8. Fluorescence spectra of the 8L, 10L, 12L, 14L, 16L, 18L and TPP.

of phenyl ring, and it has little shift to 1491 cm^{-1} in complexes, which confirmed that the metal ion has little effect on the phenyl at meso positions. The band at about 1457 cm^{-1} of porphyrin ligands is assigned to $C_\alpha-C_m$ stretch ν_3 and it does not appear in Mn complexes. Raman bands in 1300–1450 cm^{-1} are due to the out-of-phase coupled $(C_\alpha-C_\beta)/(C_\alpha-N)$ stretching modes. The 1358 and 1329 cm^{-1} bands of porphyrin ligands are assigned to the ν_4 and ν_{12} modes, respectively. The ν_4 mode of Mn complexes appears at 1370 cm^{-1}, while its ν_{12} band shifts to 1338 cm^{-1}. The 1242 cm^{-1} band of porphyrin ligands and the 1232 cm^{-1} band of Mn complexes are attributed to C_m-ph stretch ν_1. The band at 1001 cm^{-1} of porphyrin ligands is assigned to the vibration of pyrrole breathing and phenyl stretching (ν_{15}), which does not shift in Mn complexes. The band at about 964 cm^{-1} of porphyrin ligands is assigned to pyrrole breathing ν_6, but it disappeared in Mn complexes because the hydrogen atom in the N—H bonding is replaced by metal ion. The 401 and 365 cm^{-1} band of Mn complexes are assigned to the vibration of N—Mn. As we can see from Figs. 6 and 7, the band position and relative intensity of porphyrin ligands and Mn complexes with different length of side chains are almost identical, which showed that there is no structural change of porphyrin skeletons because the porphyrins have similar *para*-substituted aromatic group on the methylene bridge of porphyrins.

3.5. Fluorescence spectra

The emission spectra of porphyrin ligands and TPP in DMF obtained at an excitation wavelength of 420 nm are shown in Fig. 8, and the peak values of their emission spectral bands are given in Table 2. There are fluorescence of the S_2 (Soret band) and the S_1 (Q band) in porphyrin complexes. The fluorescence of Soret band is attributed to the transition from the second excited singlet state S_2 to the ground state S_0, which is much weaker than that of the $S_1 \rightarrow S_0$ transition of the Q band emission. Its quantum yield is so low that the fluorescence becomes unobservable in this work. Fluorescence of S_1 consists of two bands, Q (0–1) and Q (0–2). From Fig. 8, it can be seen that Q (0–1) and Q (0–2) fluorescent bands of porphyrin ligands are in the regions of 655–657 and 717–720 nm, respectively. Compared with the fluorescent bands at 653 and 715 nm of TPP, the emission peaks of porphyrin ligands have shifted to the red region. This shows that the porphyrin macrocycle conjugation is affected by the electronic donating groups. The conjugation is enhanced when the amide groups linked on the phenyl group.

The fluorescence intensities of Mn complexes are much weaker than that of the porphyrin ligands. The result is same with the reference and confirmed that the transitional metal on centre of porphyrin ring quench the fluorescence of porphyrin [25].

3.6. Thermal studies

Thermogravimetric analyses (TGA) and differential thermal analysis (DTA) curves of 12L and 12Mn are shown in Figs. 9 and 10, respectively. DTA curve of the ligand has two endothermic peaks at 240 and 276 °C and five exothermic peaks at 356, 400, 420, 478 and 520 °C, respectively. The endothermic peak at 240 °C corresponds to a 7.2% weight loss of TGA curve, which is the loss of crystalline water [26]. The endothermic peak at 276 °C of DTA curve maybe caused by the phase transition of the compound because there is no weight loss on the TGA curve. In order to confirm our conclusion, we have applied differential scanning calorimetry (DSC) to 12L. When the second heating started from room temperature to 300 °C,

Table 2
The emission spectra data of porphyrin ligands and TPP

Compounds	Solvent	λ_{ex} (nm)	Q (0−1)	Q (0−2)	Φ_f
8L	DMF	420	655	720	0.043
10L	DMF	420	656	717	0.025
12L	DMF	420	657	720	0.023
14L	DMF	420	657	721	0.019
16L	DMF	420	657	718	0.045
18L	DMF	420	656	717	0.057
TPP	DMF	420	653	715	0.110[a]

[a] Φ_f value of TPP is obtained from Ref. [24].

the DSC picture showed only one peak at about 270 °C and the peak at 240 °C disappeared (not shown in this article) because the crystalline water had lost during the first heating. The exothermic peaks are corresponding to the decomposition of the ligand. The TGA curves of the ligand have several weight-loss processes. Decomposition began at 300 °C and finished completely at 800 °C. This is a continuous decomposition process; the four small exothermic peaks are the loss of chains of porphyrin ring and the big exothermic peak at 520 °C corresponds to collapse of the porphyrin skeleton. When heated to 800 °C, the porphyrin ligand was completely decomposed and the TGA curve became smooth. For Mn complex, the DTA curve has one small endothermic peak at 232 °C and five exothermic peaks at 293, 380, 401, 470 and 525 °C, respectively. The endothermic peak corresponds to 1.1% weight loss of TGA curve, which is the lost of one crystalline water. The exothermic peak at 293 °C corresponds to a weight of 3.7%, in good agreement with the calculated 3.6% weight loss of the lost of coordinate chlorion. The decomposition of Mn complex is a continuous process too. It was decomposed completely in the range of 340−600 °C, involved the loss of side chains and the collapse of the whole porphyrin framework. After 600 °C, TGA curve became smooth and weight loss did not occur again, leaving about 7% residue of oxidate.

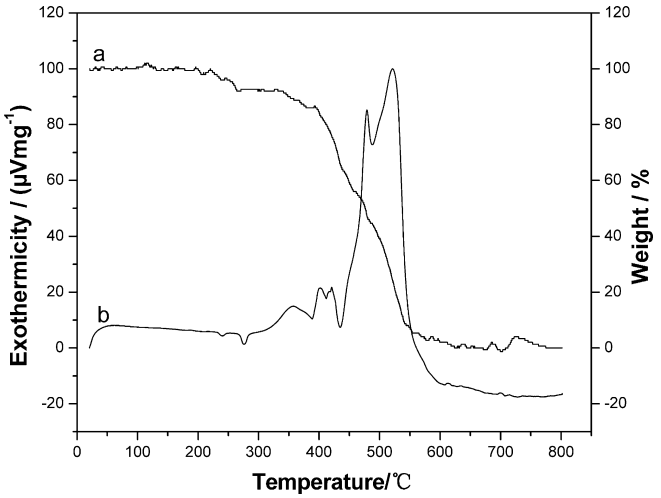

Fig. 9. TGA (a) and DTA (b) pictures of 12L.

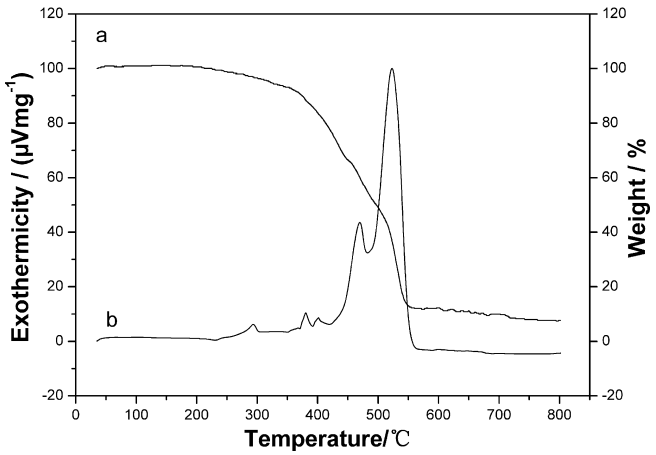

Fig. 10. TGA (a) and DTA (b) pictures of 12Mn.

3.7. Electrochemistry

Cyclic voltammograms illustrating the reduction of TPP, 8L and 8Mn in DMF, containing 0.1 mol/L TBAP as supporting electrolyte are shown in Fig. 11, and a summary of the half-wave potentials of porphyrin ligands and Mn complexes is listed in Table 3. The cyclic voltammograms of TPP and 8L are similar in shape and yield well-defined current–voltage curves for a one-electron transfer. Reactions at the electrode surface correspond to the reduction of the neutral porphyrin ring; TPP is reduced at −1.27 and −1.73 V while 8L is reduced at −1.49 and −1.94 V. The first reduction of TPP and 8L corresponds to the formation of π anion radical and the second reduction leads to the formation of porphyrin dianion. The potentials of 8L shift cathodically along the potential axis for about 220 mV compared to TPP. This can be explained by the

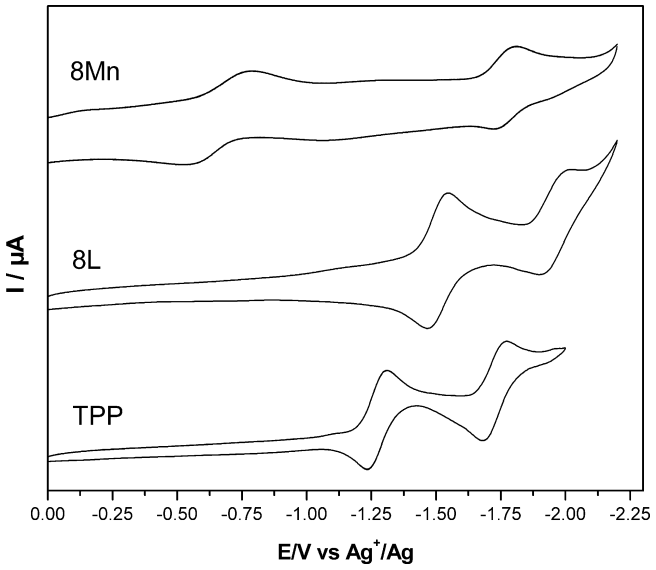

Fig. 11. Cyclic voltammograms of TPP, 8L, 8Mn in DMF + 0.1 mol/l TBAP.

Table 3
Cyclic voltammetry data of porphyrin ligands and Mn complexes

Compounds	Ered1/V	Ered2/V
TPP	−1.27	−1.73
8L	−1.49	−1.94
10L	−1.51	−1.96
12L	−1.50	−1.96
14L	−1.50	−1.96
16L	−1.51	—
8Mn	−0.65	−1.77
10Mn	−0.66	−1.78
12Mn	−0.67	−1.78
14Mn	−0.67	−1.77
16Mn	−0.67	−1.78
18Mn	−0.66	−1.76

attachment of an electron-donating group at *para* position of the four phenyl groups. The half-wave potentials would shift in a manner predicted by the Hammett linear free energy relationship $\Delta E_{1/2} = 4\sigma\rho$ [27], where σ is the total polar substituent constant which is dependent on the kind and position of the four substituents, and ρ is the reaction constant which is given in volts and expresses the susceptibility of the electrode reaction to the total polar effect of the substituents. Its value depends on the kind of electroactive group and the composition of the solvent and supporting electrolyte, as well as the temperature.

The cyclic voltammogram of 8Mn obtained in DMF is different from the ligand. Two reduction waves are obtained, the first at −0.65 V corresponds to the reaction Mn (III)/Mn (II), and the second occurs at −1.77 V and can be assigned as formation of the anion radical [28]. The peak separation of the reduction Mn (III)/Mn (II) is much larger than that of the reduction of porphyrin ring. This phenomenon could be due to the coordination of Mn porphyrin. The removal of the coordination ion during reduction should result a lower rate constant. As listed in Table 3, there are similar results for the samples whose central ions are identical except 16L and 18L because they are not soluble well in DMF. Comparing the cyclic voltammetric results of porphyrin ligands and Mn complexes, it is found that the redox potentials are almost identical when the length of side chains increased. This is probably due to the substituent constants of the alkylamido groups are almost identical and the size of porphyrin has little effect on the redox potentials.

4. Conclusion

The above experimental results indicate that only the ligands with long chains of more than 12 carbon atoms are mesogeic while the Mn complexes are not. The length of *para*-alkylamideyl group on the phenyl group has little effect on porphyrin properties. The UV−vis spectra, infrared spectra, Resonance Raman spectra, fluorescence spectra and cyclic voltammograms are almost identical. According to thermal studies, porphyrin ligand and Mn complex are stable up to nearly 300 °C, and the decomposition of the compounds is a continuous process. The fluorescent emission peaks of porphyrin ligands are red shift compared to TPP. The quantum yields are in the range of 0.019−0.057. The potentials of porphyrin ligands shift cathodically compared to TPP due to the electron-donating group at *para* position of the four phenyl groups. The cyclic voltammetry of Mn complexes is different from the porphyrin ligand, which shows not only the redox of the porphyrin ring, but also the redox of the metal ion Mn (III)/Mn (II).

References

[1] E.D. Sternberg, D. Dolphin, C. Bruckner, Tetrahedron 54 (1998) 4151.
[2] R.K. Lammi, A. Ambroise, T. Balasubramanian, R.W. Wagner, D.F. Bocian, D. Holten, J.S. Lindsey, J. Am. Chem. Soc. 122 (2000) 7579.
[3] C.A. Mirkin, M.A. Ratner, Annu. Rev. Phys. Chem. 43 (1992) 719.
[4] F. Remacle, S. Speiser, R.D. Levine, J. Phys. Chem. B 105 (2001) 5589.
[5] P.G. Van Patten, A.P. Shreve, J.S. Lindsey, R.J. Donohoe, J. Phys. Chem. B 102 (1998) 4209.
[6] R.H. Jin, Chem. Commun. (2002) 198.
[7] J.W. Goodby, P.S. Robinson, B.K. Teo, Mol. Cryst. Liq. Cryst. 56 (1980) 303.
[8] Y. Shimizu, A. Ishikawa, S. Kusabayashi, Chem. Lett. (1986) 1041.
[9] B.A. Gregg, M.A. Fox, A.J. Bard, J. Am. Chem. Soc. 111 (1989) 3024.
[10] R.P. Bimal, S.S. Kenneth, J. Am. Chem. Soc. 120 (1998) 11802.
[11] W. Liu, Y.H. Shi, T.S. Shi, Chem. Res. Chin. Univ. 20 (2004) 20.
[12] H.J. Eichhorn, J. Porphyrins, Phthalocyanines 4 (2000) 88.
[13] J.Z. Li, H. Xin, M. Li, Liq. Cryst. 33 (2006) 913.
[14] R.L. Hill, M. Goutermann, A. Ulman, Inorg.Chem. 21 (1982) 1450.
[15] D.J. Quimby, F.R. Longo, J. Am. Chem. Soc. 97 (1975) 5111.
[16] W.J. Kruper, T.A. Chamberlin, M. Kochanny, J. Org. Chem. 54 (1989) 2753.
[17] X.M. Guo, T.S. Shi, J. Mol. Struct. 789 (2006) 8.
[18] D.W. Thomas, A.E. Martell, J. Am. Chem. Soc. 78 (1956) 1338.
[19] I.K. Choi, Y. Liu, Z. Wei, M.D. Ryan, Inorg. Chem. 36 (1997) 3113.
[20] W. Liu, Y.H. Shi, T.S. Shi, Chem. J. Chin. Univ. 24 (2003) 200.
[21] G.S.S. Saini, Spectrochimica. Acta. Part A 64 (2006) 981.
[22] X.Y. Li, R.S. Czernuszewicz, J.R. Kincaid, Y.O. Su, T.G. Spiro, J. Phys. Chem. 94 (1) (1990) 31.
[23] F. Paulat, V.K.K. Praneeth, C. Nather, N. Lehnert, Inorg. Chem. 45 (2006) 2835.
[24] M.J. Gouterman, Mol. Spectrosc. 6 (1961) 138.
[25] A. Harriman, J. Chem. Soc. Faraday. Trans. I 77 (1981) 369.
[26] Z.F. Li, S.W. Wang, J.X. Wang, Chin. J. Inorg. Chem. 19 (2003) 691.
[27] K.M. Kadish, M.M. Morrison, J. Am. Chem. Soc. 98 (1976) 3326.
[28] S.L. Kelly, K.M. Kadish, Inorg. Chem. 21 (1982) 3631.